

Positive Exchange Bias between Permalloy and Twined (10 $\bar{1}$ 0)-Cr₂O₃ Films

Wei Yuan^{1,2†}, Tianyu Wang^{1,2†}, Tang Su^{1,2}, Qi Song^{1,2}, Wenyu Xing^{1,2}, Yangyang Chen^{1,2}, and
Wei Han^{1,2*}

¹International Center for Quantum Materials, Peking University, Beijing, 100871, P. R. China

²Collaborative Innovation Center of Quantum Matter, Beijing 100871, P. R. China

†These authors equally contribute to this paper.

*Correspondence to be addressed to: weihan@pku.edu.cn (W.H.)

Abstract:

We report the discovery of a positive exchange bias between Ni₈₀Fe₂₀ (Py) and twined (10 $\bar{1}$ 0)-Cr₂O₃ film near its blocking temperature (T_B) when it is cooled in an in-plane magnetic field applied along 45 degrees from the two spin configurations of the Cr atoms. This is an abnormal behavior compared to the negative exchange bias at all temperatures below T_B when the cooling and measuring magnetic fields are applied along one of the two spin configurations of the Cr atoms. We speculate these results could be related to the exchange interactions between the twined structure of the (10 $\bar{1}$ 0)-Cr₂O₃ film epitaxially grown on the rutile (001)-TiO₂ substrate.

Keywords: Exchange bias, antiferromagnetic oxide, epitaxial growth

I . INTRODUCTION

The interfacial exchange interaction between a ferromagnet (FM) and an antiferromagnet (AFM) gives rise to the exchange bias (H_{EB}), the shift of the magnetization hysteresis loop from zero magnetic field [1-4]. There has been enormous effort to explore the exchange bias for practical applications in magnetic sensors and memory devices [5]. In most cases for the FM/AFM bilayer structure, a positive cooling magnetic field gives rise to a negative H_{EB} , the shift of the magnetization hysteresis loop toward negative magnetic fields [2]. Whilst, there have been also quite a few studies reporting a positive H_{EB} at the interface of FM/AFM and several mechanisms have been proposed to account for the positive H_{EB} [6-12]. For example, magnetic ordering of the AFM spins under large cooling magnetic fields and the antiferromagnetic coupling between FM/AFM spins could give rise to a positive H_{EB} [6-8]. The net effect of a competition between exchange coupling and uniaxial magnetic anisotropy could lead to a positive H_{EB} [9,10]. Besides, a positive H_{EB} has also been observed in AFM CuMn below its spin glass transition, which is related to the Ruderman-Kittel-Kasuya-Yosida interaction [11], in (111) oriented $\text{LaNiO}_3/\text{LaMnO}_3$ superlattice, which is associated with the antiferromagnetic structure in LaNiO_3 and the presence of interface asymmetry with LaMnO_3 [12], and in the heterostructure of Co/CoO due to interfacial pinning of the AFM spins [13].

In this paper, we report the observation of a positive H_{EB} in the bilayer structure of $\text{Ni}_{80}\text{Fe}_{20}$ (Py)/(10 $\bar{1}$ 0)- Cr_2O_3 , where Cr_2O_3 is a twined film epitaxially grown on (001)- TiO_2 substrate using pulsed laser deposition. This positive H_{EB} is observed at the temperatures near the blocking temperature (T_B) of the Cr_2O_3 film and when it is cooled in an in-plane magnetic field directed along the TiO_2 [110] direction. On the other hand, if the cooling field is applied along the TiO_2

[100] direction, negative H_{EB} is observed for the whole temperature range below T_B . This unusual behavior near the blocking temperature indicates complicated spin structures due to the exchange interaction between the twined structure of the Cr_2O_3 film and Zeeman interaction associated with an off c-axis magnetic field.

II. EXPERIMENTAL DETAILS

The sample in our experiment is a multilayer structure of Al (20 nm)/Py (10 nm)/(10 $\bar{1}0$)- Cr_2O_3 (13 nm)/(001)- TiO_2 . The Cr_2O_3 is an AFM film with a twined crystalline structure grown on the rutile (001)- TiO_2 substrate using high vacuum pulsed laser deposition. The Py and Al layers are grown by magnetron sputtering, where the Al layer is used to protect the Py layer from oxidation during the measurement. Figs.1(a) and 1(b) show the *in-situ* reflection high energy electron diffraction (RHEED) patterns of the rutile TiO_2 substrate viewed along [100] and [110] directions at room temperature prior to the Cr_2O_3 growth. After the growth of 13 nm Cr_2O_3 at 350°C, the RHEED patterns at room temperature are shown in Figs. 1(c) and 1(d) viewed from the same directions as Figs. 1(a) and 1(b), respectively. Fig. 1(e) is the schematic drawing of the side view for the (10 $\bar{1}0$)- Cr_2O_3 grown on (001)- TiO_2 substrate, where the spin orientations of the Cr atoms are aligned in-plane along the TiO_2 [100] or [010] directions. The top view of the spin orientations is shown in Fig. 1(f). As there are two equivalent configurations or orientations, with a 50% probability for each, a twined crystalline Cr_2O_3 film is resulted. The detailed high-resolution transmission electron microscopy of the interface and this twined crystalline structure has been reported in our previous study [14].

The magnetic hysteresis curves of the multilayer structure are measured via Quantum Design's Magnetic Physical Measurement System (MPMS). Prior to the exchange bias

measurement, the sample is first cooled down from 350 K in an in-plane magnetic field of 1000 Oe to set the exchange bias direction. In our study, there are two measurement geometries, as shown in Figs. 2(a) and 2(b). For the first one which we refer to the 1st geometry, the applied cooling and measuring magnetic fields are along the TiO₂ [100] direction, which is also one of the two spin configurations of the Cr atoms of Cr₂O₃ film (Fig. 2(a)). For the other one which we refer to the 2nd geometry, the applied cooling and measuring magnetic fields are along the TiO₂ [110] direction, which is 45 degrees from either one of the two spin configurations of the Cr atoms of Cr₂O₃ film (Fig. 2(b)).

III. RESULTS AND DISCUSSION

A. The magnetization hysteresis measurement

Figs. 2(c) – 2(e) show the typical magnetization hysteresis loops of Py/Cr₂O₃ bilayer at 60 K, 50 K, and 30 K respectively, where the black curves indicate the measurement in the 1st geometry (Fig. 2(a)), and the red curves indicate the measurement in the 2nd geometry (Fig. 2(b)). The left (H_{LC}) and right (H_{RC}) coercive fields can be directly obtained from these curves, and the H_{EB} can be determined from $H_{EB} = (H_{LC} + H_{RC})/2$. The red/black dashed lines indicate the H_{EB} for these magnetization hysteresis loops. At the temperatures close to T_B of Cr₂O₃, there is a distinct difference between the two measurement geometries. A normal negative H_{EB} is observed in the 1st geometry (black curves in Figs. 2(c) and 2(d)). Whilst, an interesting positive H_{EB} is observed only in the 2nd measurement geometry (red curves in Figs. 2(c) and 2(d)).

As the temperature decreases further down below 40 K, the magnetization hysteresis loops are almost identical for both measurement geometries. Representative curves measured at 30 K are shown in Fig. 2(e).

B. Temperature dependence of the coercive fields and H_{EB}

Fig. 3(a) shows both H_{LC} (black squares) and H_{RC} (red squares) as a function of the temperature measured in the 1st geometry. As the temperature decreases, the absolute values of both H_{LC} and H_{RC} show a sharp increase below the temperature of ~ 70 K. For the 1st geometry, the absolute value of H_{RC} is smaller than that of H_{LC} , which means that the H_{EB} is negative for all the temperatures below T_B . For the 2nd geometry, both the absolute values of H_{LC} (black squares) and H_{RC} (blue squares) show a sharp increase below the temperature of ~ 70 K, as shown in Fig. 3 (b). Different from the 1st geometry, a much sharper increase of the H_{RC} is observed in the 2nd geometry, giving rise to a positive H_{EB} close to the T_B .

Fig. 3(c) summarizes the H_{EB} as a function of the temperature for both two measurement geometries where the cooling and measuring magnetic fields are along the TiO_2 [100] (black squares) and [110] (blue balls) directions. Clearly, a T_B of ~ 70 K is determined for this 13 nm Cr_2O_3 film from both measurement geometries. The measured T_B is much lower compared to the value reported on (0001) oriented bulk Cr_2O_3 single crystals [15], which could be associated with the trivial finite-size effects [2,16-18] and some non-trivial finite-size effects related to the crystal defects in the Cr_2O_3 film [19]. Most interestingly, a positive H_{EB} is observed at 50, and 60 K when the cooling and measuring magnetic fields are along the TiO_2 [110] direction (blue balls).

C. H_{EB} measurement along the TiO_2 [010] and $[1\bar{1}0]$ directions

As there are two crystalline zones in $(10\bar{1}0)$ oriented Cr_2O_3 , we also measure H_{EB} by cooling the magnetic field along the TiO_2 [010] and $[1\bar{1}0]$ directions. Fig. 4(a) shows the temperature dependence of H_{EB} by cooling the magnetic field along the TiO_2 [100] and [010] directions.

Almost identical exchange biases are observed at each temperature. Fig. 4(b) shows the temperature dependence of H_{EB} by cooling the magnetic field along the TiO_2 [110] and $[\bar{1}\bar{1}0]$ directions. Very similarly, a positive H_{EB} is observed at the temperatures that are close to the T_B .

D. Cooling magnetic field strength effect on H_{EB}

Next, the effect of cooling magnetic field strength on the H_{EB} is studied. Fig. 5(a) and 5(b) show the temperature dependence of H_{EB} under different cooling magnetic field strengths, for the magnetic fields along the TiO_2 [100] and [110] directions, respectively. First of all, the magnitude of the cooling magnetic fields has a negligible effect on the H_{EB} at higher temperatures, and a larger cooling magnetic field leads to a lower value of the H_{EB} at lower temperatures, which could be associated with the spin structure at the interface induced by the cooling magnetic field [7]. Second of all, the positive exchange bias is not affected at all by the large magnetic field up to 70000 Oe, indicating the negligible role from the magnetic field strength.

E. Possible explanation for the positive H_{EB}

Both the temperature and cooling magnetic field strength dependences of the H_{EB} indicate that the positive H_{EB} is related to the twined structure of the $(10\bar{1}0)\text{-Cr}_2\text{O}_3$ film grown on rutile (001)- TiO_2 substrate. To study this, we analyze the H_{EB} using numerical calculation based on the coherent rotation model (Stoner-Wohlfarth type) [20], which has been used to explain the positive H_{EB} resulting from the competition between shape anisotropy and the exchange interaction of the heterostructure [9,10]. If we simply neglect the interaction between the spin orientations of the two twined structures in Cr_2O_3 , the free energy (f) can be described as:

$$f = -HM_s \cos\theta - K_{E1} \cos(\theta - \theta_{E1}) - K_{E2} \cos(\theta - \theta_{E2}) - K_u \cos^2(\theta - \theta_u) \quad (1)$$

where H is the external magnetic field, M_s is the saturation magnetization, K_u is the uniaxial anisotropy, K_{E1} and K_{E2} are the unidirectional anisotropies of the two different twined structures, θ is the angle between H and the FM magnetization, θ_{E1} and θ_{E2} are the angles between the H and the unidirectional anisotropic axes of the twined Cr_2O_3 film, and θ_u is the angle between H and the uniaxial axis of FM layer.

Our numerical simulation shows that the H_{EB} is always negative by cooling the magnetic fields along the TiO_2 [100] and [010] directions, which are consistent with our experimental results. For the numerical simulation of the H_{EB} by cooling and applying the external magnetic fields along the TiO_2 [110] and $[\bar{1}\bar{1}0]$ directions, we can't reproduce the positive H_{EB} near T_B . There could be two mechanisms to account for this behavior. The first one is related to the respective magnetic domains sizes of the FM and AFM layers [21,22]. If the twined regions of AFM are large enough, the Py on top may have different magnetization directions, which would be equivalent to dropping one of the K_E terms in equation (1). As the temperature changes close to T_B , the ratio of K_E/K_u could give rise to a positive exchange bias similar to previous report [9]. However, we do not observe a double magnetic hysteresis as shown in ref [21,22], thus, the direct imaging of the magnetic domains would be necessary to test this mechanism. The second mechanism could be relate to the interaction between the two twined structures that is simply neglected in equation (1). This unusual behavior near the blocking temperature indicates complicated spin structures as a result of weak exchange interaction and Zeeman interaction associated with an off c-axis magnetic field. Future theoretical studies are needed to fully understand this behavior.

IV. CONCLUSION

We report a positive H_{EB} near the blocking temperature of the $(10\bar{1}0)$ - Cr_2O_3 film, when the magnetic field is applied along 45 degrees between the two sets of spin configurations of the Cr atoms. This observation indicates complicated spin structures at the interface between Py and twined $(10\bar{1}0)$ - Cr_2O_3 film near its T_B .

Acknowledgements

We acknowledge the fruitful discussion with Dr. Axel Hoffmann and Prof. Jing Shi, and the funding support of National Basic Research Programs of China (973 Grants 2014CB920902, 2015CB921104, and 2013CB921903) and the National Natural Science Foundation of China (NSFC Grant 11574006). Wei Han also acknowledges the support by the 1000 Talents Program for Young Scientists of China.

References:

- [1] W. H. Meiklejohn and C. P. Bean, Phys. Rev. **105**, 904 (1957).
- [2] J. Nogués and I. K. Schuller, J. Magn. Magn. Mater. **192**, 203 (1999).
- [3] M. Kiwi, J. Magn. Magn. Mater. **234**, 584 (2001).
- [4] F. Radu and H. Zabel, *Exchange Bias Effect of Ferro-/Antiferromagnetic Heterostructures* (Springer Berlin Heidelberg, 2008), Springer Tracts in Modern Physics, 227, 97-184.
- [5] S. S. P. Parkin, K. P. Roche, M. G. Samant, P. M. Rice, R. B. Beyers, R. E. Scheuerlein, E. J. O'Sullivan, S. L. Brown, J. Bucchigano, D. W. Abraham, Y. Lu, M. Rooks, P. L. Trouilloud, R. A. Wanner, and W. J. Gallagher, J. Appl. Phys. **85**, 5828 (1999).
- [6] J. Nogués, D. Lederman, T. J. Moran, and I. K. Schuller, Phys. Rev. Lett. **76**, 4624 (1996).

- [7] C. Leighton, J. Nogués, B. J. Jönsson-Åkerman, and I. K. Schuller, *Phys. Rev. Lett.* **84**, 3466 (2000).
- [8] H. Ohldag, H. Shi, E. Arenholz, J. Stöhr, and D. Lederman, *Physical Review Letters* **96**, 027203 (2006).
- [9] S. H. Chung, A. Hoffmann, and M. Grimsditch, *Phys. Rev. B* **71**, 214430 (2005).
- [10] A. K. Suszka, O. Idigoras, E. Nikulina, A. Chuvilin, and A. Berger, *Phys. Rev. Lett.* **109**, 177205 (2012).
- [11] M. Ali, P. Adie, C. H. Marrows, D. Greig, B. J. Hickey, and R. L. Stamps, *Nat. Mater.* **6**, 70 (2007).
- [12] M. Gibert, M. Viret, P. Zubko, N. Jaouen, J. M. Tonnerre, A. Torres-Pardo, S. Catalano, A. Gloter, O. Stephan, and J. M. Triscone, *Nat. Commun.* **7** (2016).
- [13] T. Gredig, I. N. Krivorotov, P. Eames, and E. D. Dahlberg, *Appl. Phys. Lett.* **81**, 1270 (2002).
- [14] W. Yuan, T. Su, Q. Song, W. Xing, Y. Chen, T. Wang, Z. Zhang, X. Ma, P. Gao, J. Shi, and W. Han, *Scientific Reports* **6**, 28397 (2016).
- [15] X. He, Y. Wang, N. Wu, A. N. Caruso, E. Vescovo, K. D. Belashchenko, P. A. Dowben, and C. Binek, *Nat. Mater.* **9**, 579 (2010).
- [16] T. Ambrose and C. L. Chien, *Phys. Rev. Lett.* **76**, 1743 (1996).
- [17] K.-i. Imakita, M. Tsunoda, and M. Takahashi, *J. Appl. Phys.* **97**, 10K106 (2005).
- [18] J. Wu, J. S. Park, W. Kim, E. Arenholz, M. Liberati, A. Scholl, Y. Z. Wu, C. Hwang, and Z. Q. Qiu, *Phys. Rev. Lett.* **104**, 217204 (2010).
- [19] X. He, W. Echtenkamp, and C. Binek, *Ferroelectrics* **426**, 81 (2012).
- [20] E. C. Stoner and E. P. Wohlfarth, *Philos. Trans. R. Soc. London, Ser. A* **240**, 599 (1948).
- [21] I. V. Roshchin, O. Petravic, R. Morales, Z. P. Li, X. Batlle, and I. K. Schuller, *Eur. Phys. Lett.* **71**, 297 (2005).
- [22] S. Brück, J. Sort, V. Baltz, S. Suriñach, J. S. Muñoz, B. Dieny, M. D. Baró, and J. Nogués, *Adv. Mater.* **17**, 2978 (2005).

Figure Captions

Figure 1: (a-b) RHEED patterns of rutile TiO_2 substrate viewed along the $[100]$ and $[010]$ directions, respectively. (c-d) RHEED patterns of the twined $(10\bar{1}0)$ - Cr_2O_3 film (thickness: 13 nm) viewed from TiO_2 $[100]$ and $[110]$ directions. (e) The schematic drawing showing the side view of the atomic interface between Cr_2O_3 and TiO_2 . The red dashed line indicates the interface between Cr_2O_3 and TiO_2 , and the black dashed line indicates the crystalline boundary of the twined Cr_2O_3 film. (f) The schematic drawing showing the top view of the twined Cr_2O_3 film. The spins of the Cr atoms are indicated by the red arrows.

Figure 2: (a-b) Schematic drawings of the in-plane exchange bias measurement between Py and the twined Cr_2O_3 with the magnetic field applied along TiO_2 $[100]$ (a; 1st geometry) and $[110]$ (b; 2nd geometry) directions. (c-e) The magnetization curves of Py measured as a function of the in-plane magnetic field at 60K, 50K, and 30K, respectively. The red/black curves indicate the measurement with the magnetic fields applied along TiO_2 $[110]/[100]$ direction. The red/black dashed lines are the guide lines for H_{EB} .

Figure 3: (a-b) Left (H_{LC}) and right (H_{RC}) coercive fields of Py as a function of the temperature for the magnetic fields applied along TiO_2 $[100]$ and $[110]$ directions, respectively. (c) Temperature dependence of H_{EB} between Py and Cr_2O_3 for the magnetic fields applied along TiO_2 $[100]$ and $[110]$ directions, respectively. The dashed magenta line is the guide line for zero H_{EB} .

Figure 4: (a) Temperature dependence of H_{EB} between Py and Cr_2O_3 for the magnetic fields applied along TiO_2 $[100]$ and $[010]$ directions, respectively. (b) Temperature dependence of H_{EB}

between Py and Cr₂O₃ for the magnetic fields applied along TiO₂ [110] and [1 $\bar{1}$ 0] directions, respectively. The dashed magenta lines are the guide lined for zero H_{EB}.

Figure 5: (a) Temperature dependence of H_{EB} between Py and Cr₂O₃ under cooling magnetic fields of 1000 (black) and 70000 Oe (red) for the magnetic fields applied along TiO₂ [100] direction. (b) Temperature dependence of the H_{EB} between Py and Cr₂O₃ under cooling magnetic fields of 1000 (black), 30000 (green), and 70000 Oe (blue), respectively, for the magnetic fields applied along TiO₂ [110] direction. The dashed magenta lines are the guide lined for zero H_{EB}.

Figure 1

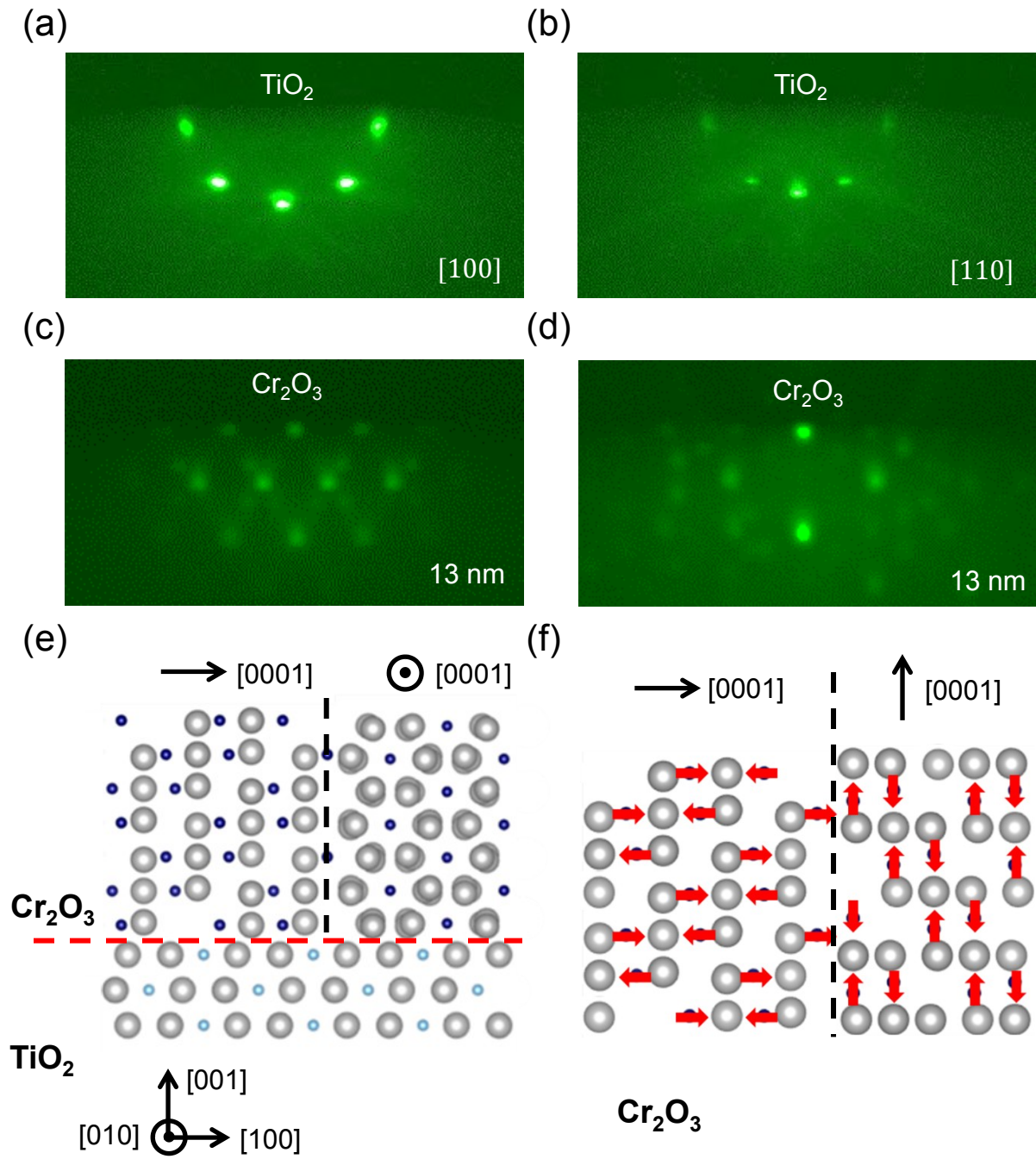


Figure 2

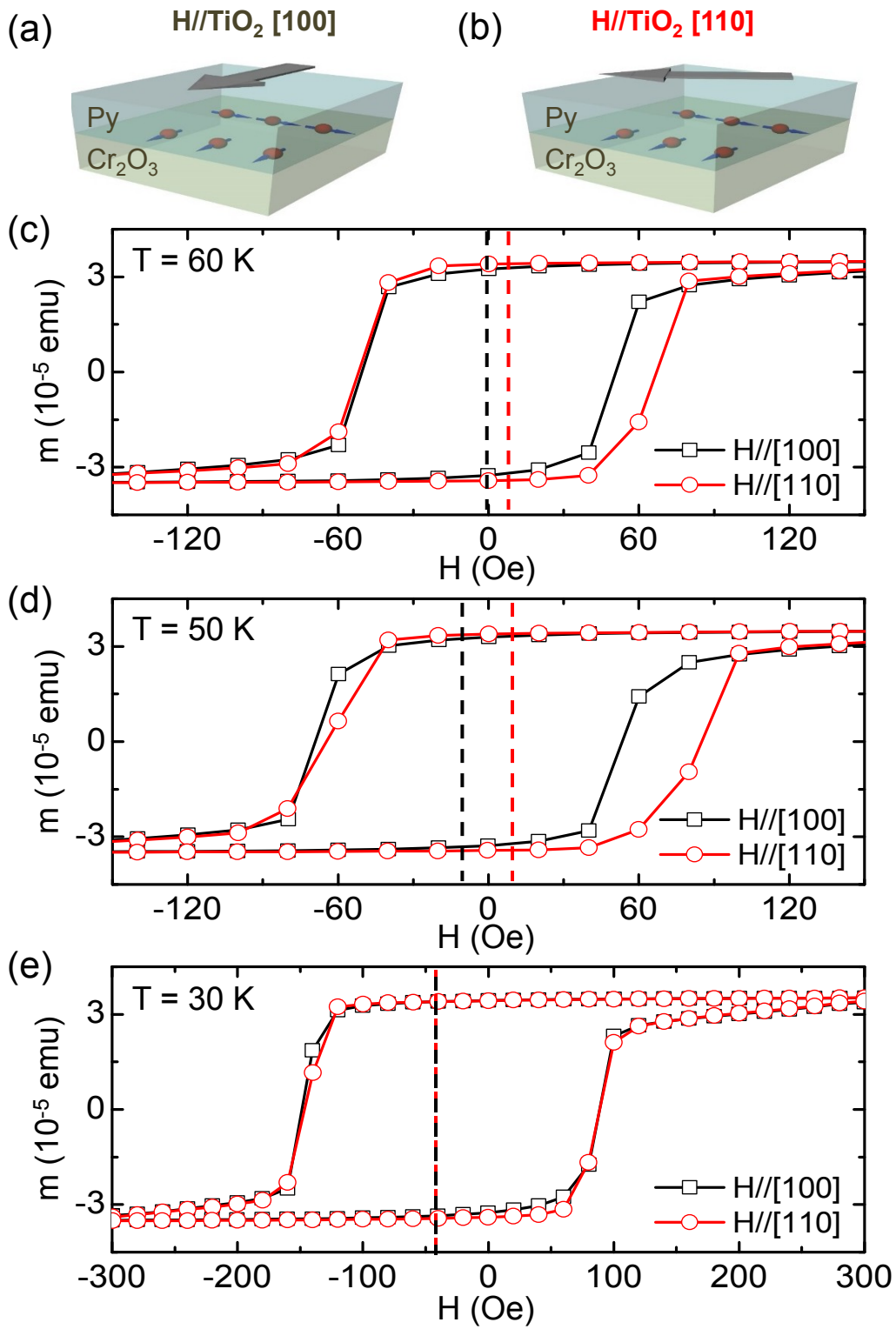


Figure 3

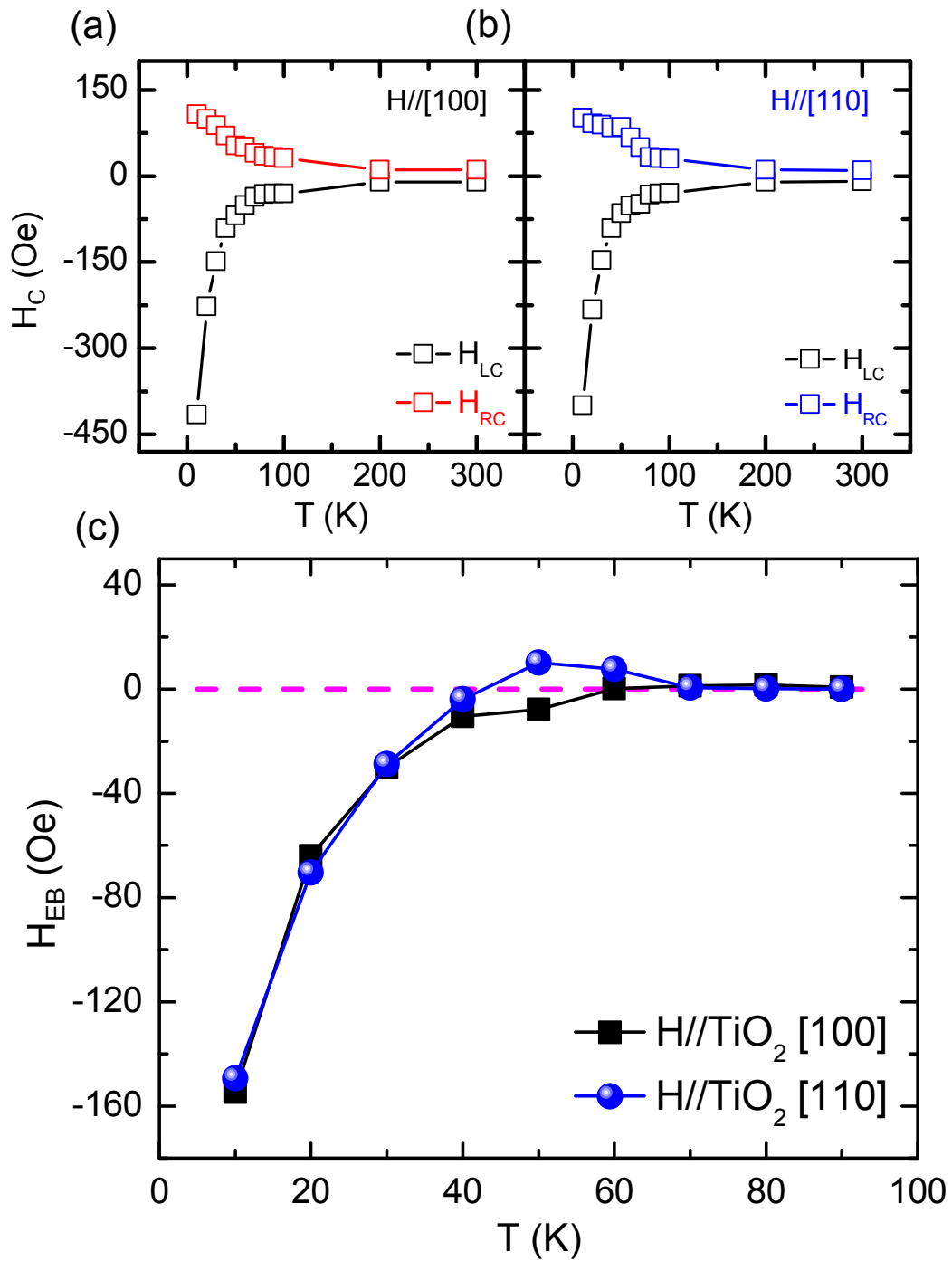


Figure 4

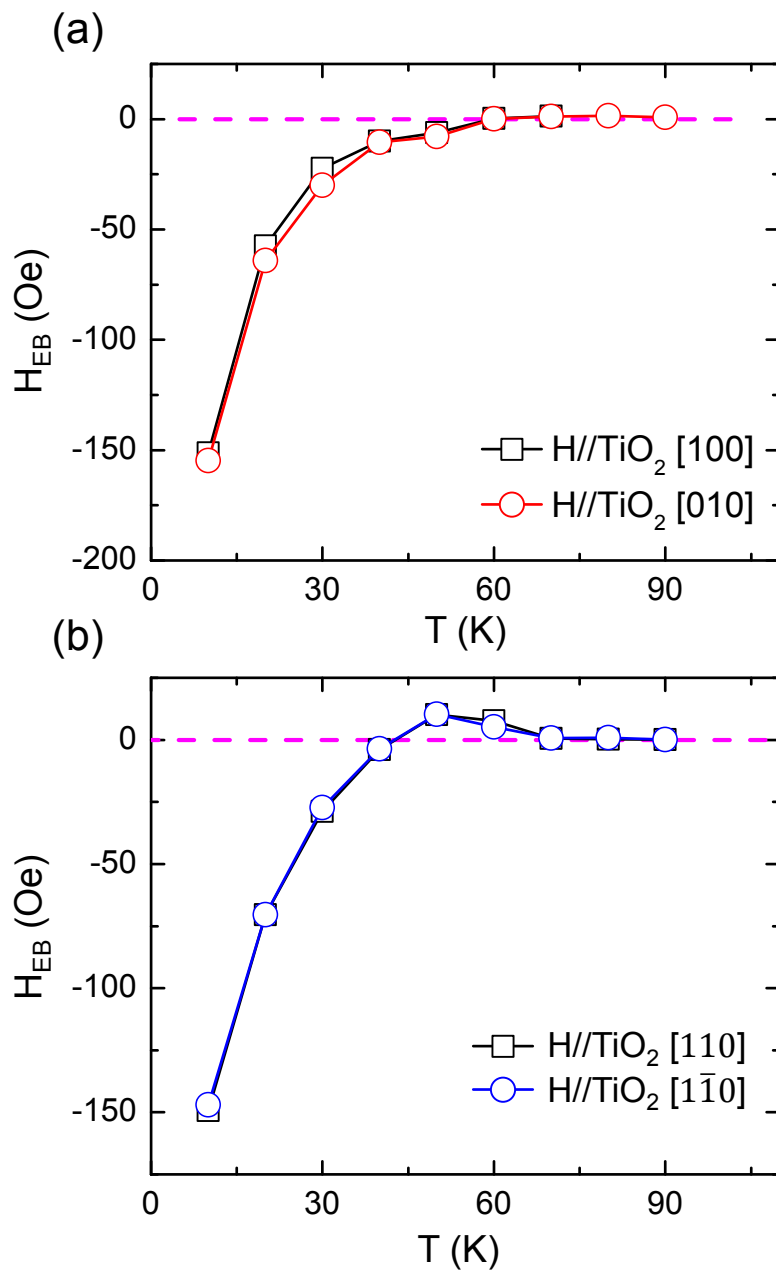


Figure 5

